

Quiescent Thermal Emission from the Neutron Star in Aql X-1

Robert E. Rutledge¹, Lars Bildsten², Edward F. Brown³, George G. Pavlov⁴,
and Vyacheslav E. Zavlin⁵

ABSTRACT

We report on the quiescent spectrum measured with *Chandra*/ACIS-S of the transient, type-I X-ray bursting neutron star Aql X-1, immediately following an accretion outburst. The neutron star radius, assuming a pure hydrogen atmosphere and hard power-law spectrum, is $R_\infty = 13.4^{+5}_{-4}$ ($d/5$ kpc) km. Based on the historical outburst record of *RXTE*/ASM, the quiescent luminosity is consistent with that predicted by Brown, Bildsten and Rutledge from deep crustal heating, lending support to this theory for providing a minimum quiescent luminosity of transient neutron stars. While not required by the data, the hard power-law component can account for $18 \pm 8\%$ of the 0.5-10 keV thermal flux. Short-timescale intensity variability during this observation is less than 15% rms (3σ ; 0.0001-1 Hz, 0.2-8 keV). Comparison between the *Chandra* spectrum and three X-ray spectral observations made between Oct 1992 and Oct 1996 find all spectra consistent with a pure H atmosphere, but with temperatures ranging from 145–168 eV, spanning a factor of 1.87 ± 0.21 in observed flux. The source of variability in the quiescent luminosity on long timescales (greater than years) remains a puzzle. If from accretion, then it remains to be explained why the quiescent accretion rate provides a luminosity so nearly equal to that from deep crustal heating.

Subject headings: stars: atmospheres — stars: individual (Aql X-1) — stars: neutron — x-rays: binaries

¹ Space Radiation Laboratory, California Institute of Technology, MS 220-47, Pasadena, CA 91125; rutledge@srl.caltech.edu

² Institute for Theoretical Physics and Department of Physics, Kohn Hall, University of California, Santa Barbara, CA 93106; bildsten@itp.ucsb.edu

³ Enrico Fermi Institute, University of Chicago, 5640 South Ellis Ave, Chicago, IL 60637; brown@flash.uchicago.edu

⁴ The Pennsylvania State University, 525 Davey Lab, University Park, PA 16802; pavlov@astro.psu.edu

⁵ Max-Planck-Institut für Extraterrestrische Physik, D-85740 Garching, Germany; zavlin@xray.mpe.mpg.de

1. Introduction

Brown, Bildsten & Rutledge (1998, BBR98 hereafter) showed that the core of a transiently accreting neutron star (NS), such as Aql X-1 (for reviews of transient neutron stars, see Chen et al. 1997; Campana et al. 1998a), is heated by nuclear reactions deep in the crust during the accretion outbursts. The core is heated to a steady-state in $\sim 10^4$ yr (see also Colpi et al. 2000), after which the NS emits a thermal luminosity in quiescence of (BBR98)

$$L_q = 8.7 \times 10^{33} \left(\frac{\langle \dot{M} \rangle}{10^{-10} M_\odot \text{yr}^{-1}} \right) \frac{Q}{1.45 \text{MeV}/m_p} \text{ ergs s}^{-1}, \quad (1)$$

where $\langle \dot{M} \rangle$ is the time-averaged mass-accretion rate onto the NS, and Q is the amount of heat deposited in the crust per accreted nucleon (Haensel & Zdunik 1990; see Bildsten & Rutledge 2000 for a discussion).

Aql X-1 has been detected in X-ray quiescence five times: once with the *ROSAT*/HRI and twice with *ROSAT*/PSPC (Verbunt et al. 1994), once with *ASCA* (Asai et al. 1998), and once with *BeppoSAX* (Campana et al. 1998b, C98 hereafter). We report in this *Letter* the detection and CCD X-ray spectroscopy of a *Chandra* observation of Aql X-1 in quiescence, and compare its luminosity and spectrum to three of these previous observations. We show that the quiescent X-ray spectrum is consistent with thermal emission from a pure H atmosphere on the NS (Rajagopal & Romani 1996; Zavlin et al. 1996), as is observed from this and other transient neutron stars in quiescence (Rutledge et al. 1999; 2000; 2001). As pointed out by BBR98, for accretion rates $\lesssim 2 \times 10^{-13} M_\odot \text{yr}^{-1}$, gravity stratifies metals in the NS atmosphere faster than they can be provided by accretion (Bildsten, Salpeter, & Wasserman 1992), making a pure H atmosphere the appropriate description of the NS photosphere.

Callanan, Filippenko & Garcia (1999) recently showed that the optical counterpart to Aql X-1 is a faint star near the previously mis-identified counterpart. This led to the counterpart’s identification as a late type star (spectral type K7 to M0) with a quiescent magnitude $V = 21.6$ at a reddening of $A_V \approx 1.6$ (Chevalier et al. 1999). The orbital period has been well measured at $P_{\text{orb}} = 18.95$ hr via photometric observations both in outburst (Chevalier & Ilovaisky 1998; Garcia et al. 1999) and quiescence (Welsh et al. 2000).

Chevalier et al. (1999) estimated the distance to the binary as 2.5 kpc by assuming that the counterpart was a main sequence star of spectral type K7, or roughly $M_c \approx 0.6 M_\odot$ and $R_c \approx 0.6 R_\odot$. However, the steady mass transfer and ellipsoidal variations (Welsh et al. 2000) require that the companion be Roche-lobe filling, which gives $R_c \approx 1.65 R_\odot (M_c/M_\odot)^{1/3}$, larger than Chevalier et al.’s estimate. If we use the de-reddened quiescent V magnitude,

we find that the distance to the binary is $d = 4.7(6.4)$ kpc (for spectral type K7) for $M_c = 0.5(1.0)M_\odot$. For a spectral type of M0, we find $d = 4(5)$ kpc for $M_c = 0.5(1.0)M_\odot$. Thus, the clear minimum distance is 4 kpc, and the current uncertainties allow for a distance as large as 6.5 kpc. The Type I bursts observed by Czerny, Czerny and Grindlay (1987) had peak fluxes of $\approx 7 \times 10^{-8}$ erg cm $^{-2}$ s $^{-1}$, which gives the solar abundance Eddington luminosity of 2×10^{38} erg s $^{-1}$ at $d = 5$ kpc. We use 5 kpc as our fiducial distance.

In § 2, we describe the *Chandra* observation and the constraints on variability during the observation. Section 3 shows our results on the spectral analysis and compares the *Chandra* observations to previous quiescent observations. We conclude §3 with a comparison of the observed luminosity to that predicted by equation (1). We discuss these results in the context of alternate emission mechanisms in § 4.

2. Chandra Observations and Timing Analysis

Aql X–1 was observed with *Chandra* (Weisskopf 1988) using the ACIS-S3 detector in imaging mode, beginning Nov 28 2000, 10:51:35 UT, 7 days after the last 1-day detection (3σ , ≈ 20 mCrab) with RXTE/ASM (Levine et al. 1996) during the outburst.

The X-ray source position was offset 4' from the optical-axis to mitigate pileup. The observation had a total exposure time of 6627.6 s over a period of 7307.6 sec (90% livetime), with time resolution of 0.44104 sec, and a 0.4 sec exposure. One X-ray source is detected in the field, at a position (based on spacecraft pointing) $\alpha = 19\text{h}11\text{m}16.00\text{s}$, $\delta = 00\text{d}35\text{m}06.4\text{s}$ (J2000), with systematic errors dominating the uncertainty of position ($\pm 1''$), consistent with the known optical position of Aql X–1 (Thorstensen et al. 1978; Callanan et al. 1999).

The data were analyzed using the CIAO v2.0 ⁶ and XSPEC v11 (Arnaud 1996). X-ray source counts were extracted within an area 10 pixels in radius about the source position, with a total of 1243 counts. At 0.075 counts/frame, the pileup fraction is $< 3\%$ and can be neglected. Background was taken from an annulus centered on the source position, with radii of 13 and 50 pixels. The expected number of background counts in the source region is 8 counts, which are neglected in our analyses.

We binned the 0.2–8 keV counts into three light curves with three different time resolutions: $\delta T = 0.44104$ s, 10 s, and 100 s. In each case, the distribution of the number of counts per bin was consistent with a Poissonian distribution, for an average number of counts per bin of $(1237 \text{ counts}) / (7308 \text{ s} / \delta T)$. We also produced a power density spectrum

⁶<http://asc.harvard.edu/ciao2.0/>

(PDS), beginning with a lightcurve of all the counts in the source region with time resolution of 0.44104 sec, producing a 0.00014-1.13 Hz PDS. The PDS is statistically consistent with a constant power at the Poisson level, and shows no evidence of any excess variability. Fitting the PDS with a power-law component with a fixed slope ($\propto \nu^{-1}$) above a (fixed) Poisson level gives a 3σ upper-limit to the root-mean-square variability of $<15\%$ (0.0001-1 Hz; 0.2-8 keV). We thus find no evidence of intensity variability during the *Chandra* observation.

3. Spectral Analysis

We binned the data into 13 energy bins (0.5-8.0 keV), and fit several single component spectral models (powerlaw, H atmosphere, Raymond-Smith, multicolor disk or blackbody). We also include H atmosphere with a power-law, with two fixed values for the power-law slope ($\alpha = 1$, $\alpha = 2$). Galactic absorption ($N_{\text{H}}=10^{22} N_{\text{H},22}\text{cm}^{-2}$) is initially left as a free parameter. The best-fit models were all statistically acceptable, and most gave column densities consistent with $A_{\text{V}} = 1.6$, and $N_{\text{H},22}=0.179 A_{\text{V}}$ (Gorenstein 1975; Predehl & Schmitt 1995); the parameters are given in Table 1.

The Raymond-Smith spectrum has a metallicity substantially below the solar value ($Z < 5 \times 10^{-3} Z_{\odot}$). In addition, Bildsten and Rutledge (2000) showed that the quiescent X-ray-to-optical flux ratio of Aql X-1 ($\sim 10^{0.5 \pm 0.2}$) is much greater than the maximum observed from quiescent stellar coronae ($F_{\text{X}}/F_{\text{opt}} \lesssim 10^{-3}$), so we exclude the stellar coronae as a possible solution. The single power-law spectrum requires a higher column density than the optically implied value ($N_{\text{H},22}=0.72$ vs. 0.30) and is much steeper (photon slope $\alpha=4.1$) than is typically observed from non-thermal X-ray sources. We reject the model on this basis.

Standard Shakura-Sunyaev (Shakura & Sunyaev 1973) disks have largely been excluded as the dominant emission of transients in quiescence (McClintock et al. 1995), although recent interest in alternative disk models (Nayakshin & Svensson 2001) suggest it is useful to constrain parameters for a multicolor disk model. And, although black-body emission does not physically describe the emergent spectrum from a transient neutron star atmosphere in quiescence (BBR98), we include these spectral parameters as well for the interested reader. Neither R_{in} of the multicolor disk model nor R_{∞} of the blackbody model appear to correspond to any physically interesting values; both are smaller than canonical NS radii.

The simplest interpretation of the spectrum is thermal emission from a pure Hydrogen atmosphere on the NS, and so we include the best-fit parameters in Table 1. However, previous observations have found a power-law component which dominates the quiescent

spectrum at high energies in Aql X–1 (Campana et al. 1998b), and in the transient Cen X–4 (Asai et al. 1996b; Campana et al. 2000; Rutledge et al. 2001), with values between $\alpha = 1$ and 2. We included a power-law component, with slope fixed alternately at $\alpha = 1$ and $\alpha = 2$. An F-test (Press et al. 1995) shows that the additional spectral component does not significantly improve the model fit (prob=0.07 and 0.13, respectively). The resulting values of R_∞ are systematically higher, while $kT_{\text{eff},\infty}$ is systematically lower, indicating that the presence of a weak power-law may be biasing the pure H atmosphere spectral model parameters. We therefore prefer the values from the H atmosphere plus $\alpha = 1$ spectral model (over the H atmosphere spectral model alone), of $R_\infty=13.4^{+5}_{-4}$ km and $kT_{\text{eff},\infty}=135^{+18}_{-12}$ eV. These are not significantly different from those of the $\alpha = 2$ spectral model.

When we hold $N_{\text{H},22}$ fixed at its best-fit value, we obtain (for the $\alpha = 1$ spectrum) $R_\infty=13.4\pm 2.0$ km and $kT_{\text{eff},\infty}=135^{+10}_{-9}$ eV, indicating that the uncertainty in N_{H} has a modest effect on the uncertainty in the H atmosphere spectral parameters.

Here $kT_{\text{eff},\infty}$ and R_∞ are the effective temperature and NS radius as measured by a distant observer. They obey the relation $L_{\text{bol}}^\infty = 4\pi R_\infty^2 \sigma T_{\text{eff},\infty}^4$, where L_{bol}^∞ is the luminosity measured by a distant observer. The “proper” values of kT_{eff} and R are related to those at infinity through the gravitational redshift parameter $g_r = [1 - 2GM/(Rc^2)]^{1/2}$ (the redshift is $1 + z = g_r^{-1}$); for a neutron star of mass $1.4 M_\odot$ and radius 10 km, $g_r = 0.766$. The gravitational field redshifts photon energies and bends their trajectories, so that $kT_{\text{eff}}=kT_{\text{eff},\infty} g_r^{-1}$ and $R=R_\infty g_r$. The observed and proper bolometric luminosities are then related by $L_{\text{bol}}^\infty = L_{\text{bol}} g_r^2$; one power of g_r accounts for the energy redshift and the other accounts for the time dilation. The observed bolometric thermal flux is then $F_{\text{bol}}^\infty=2.5\times 10^{-12}$ erg cm $^{-2}$ s $^{-1}$.

3.1. Comparison to Previously Measured Quiescent Spectra

We simultaneously fit the *Chandra* spectrum with three energy spectra taken in quiescence: *ROSAT*/PSPC in October 1992, *ROSAT*/PSPC in March 1993, and *ASCA* in October 1996 (cf. Table 2; see Rutledge et al. 1999 for details on these spectra). We included a 4% systematic uncertainty, to allow for differing calibrations between instruments. The results of these spectral fits are in Table 3).

Fitting an absorbed, pure H atmosphere spectrum with all identical parameters produces a statistically unacceptable fit ($\chi_\nu^2/\text{dof}=2.63/67$ dof; here and elsewhere in this paper, the first number is the reduced χ^2 value, the second number is the number of

degrees of freedom, and the two are separated by the backslash character). However, acceptable fits are found if we permit either N_{H} (marginally), $kT_{\text{eff},\infty}$ or R_{∞} to vary between the four observations. The observed 0.5-10 keV fluxes span a range of a factor 1.87 ± 0.21 (90% confidence). Therefore, while the spectra are statistically different, we are unable to observationally discern which spectral parameter (or combination of parameters) is changing.

We then added the power-law component. The best fit spectrum in which all five spectral parameters are the same for the four different observations was statistically unacceptable ($\chi^2_{\nu}=2.80/65$ dof; prob= 2×10^{-13}), indicating spectral variability. Acceptable fits are found if we let any of the four parameters ($N_{\text{H},22}$, $kT_{\text{eff},\infty}$, R_{∞} , $F_{X,PL}$) vary independently between the four observations. The constraints on the power-law slope are very weak. Also, in the fit in which $F_{X,PL}$ was permitted to vary, the value $\alpha = 3.5 \pm 0.5$ is steeper than is typical of these sources, combined with a high value of N_{H} .

We examined the temperature decrease as a function of time since the outburst end. Table 2 gives the time-delay between the quiescent observation and the end of the previous outburst; Table 3 contains the temperatures measured during the quiescent observation. For the 1993 *ROSAT* observation, we assumed that the outburst ended 60 days after its start. A linear fit to the data finds a temperature which decreases (-50 ± 90) eV/yr (consistent with no decrease), with a 3σ upper-limit of <270 eV/yr. This is an uncertain measurement for a number of reasons: the number of days since outburst start is uncertain by ~ 7 days, the duration of outbursts varies from outburst to outburst, and the initial temperature of the NS atmosphere may be related to the total fluence of the most recent outburst, which is unknown for 2 of the 4 outbursts. Moreover, the temperatures taken alone are not significantly different. This level of decrease is consistent with the limit on the decrease in the thermal temperature of Cen X-4, which is (-2.2 ± 1.8) eV/yr (Rutledge et al. 2001).

3.2. Power-law/Thermal Flux Ratio

C98 reported a power-law component that dominates the X-ray spectrum at energies above ≈ 2 keV in quiescence, similar to a power-law component seen in Cen X-4 (Asai et al. 1996b; Asai et al. 1998; Campana et al. 2000; Rutledge et al. 2001). As we find above, the *Chandra* spectrum does not require an additional power-law component at high energies, although inclusion of a power-law component makes a systematic difference to the parameters of the thermal component. We stress, therefore, that the power-law flux values we discuss in this section are merely the best-fit values, and are not evidence that the power-law component is present.

The best-fit power-law/thermal luminosity ratio is $18 \pm 8\%$ ($26 \pm 13\%$) for a fixed $\alpha = 1$ ($\alpha = 2$; see Table 1). The best-fit power-law flux is $(2.2 \pm 1) \times 10^{-13}$ [$(3.1^{+1.6}_{-1.4}) \times 10^{-13}$] $\text{erg cm}^{-2} \text{s}^{-1}$ for $\alpha = 1$ [$\alpha = 2$] in the 0.5-10 keV pass band. These are consistent with power-law flux reported in quiescence from the observations of C98 ($5 \times 10^{-13} \text{ erg cm}^{-2} \text{s}^{-1}$).

We investigated if a variable power-law intensity could be responsible for the variations between the four observations. We held the value of $\alpha=1$ fixed (the value found by C98 in observations 3-6), kept the N_{H} , $kT_{\text{eff},\infty}$, and R_{∞} constant between the four observations, and permit the power-law flux to vary between observations. The best fit was unacceptable ($\chi^2_{\nu}/\text{dof}=1.64/65$ dof; prob= 8×10^{-4}). We conclude that the observed spectral variability cannot be explained by a variable power-law component with the slope observed by C98. The variability is caused either by a power-law which changes in slope and flux, or variability in the thermal component or column density.

3.3. Predicted versus Observed Quiescent Flux

Aql X–1 is one of the brightest known quiescent NSs, and, combined with its frequent accretion outbursts, provides the best opportunity to test the relationship between the time-averaged outburst flux and the quiescent flux predicted by BBR98.

We use the RXTE/ASM data to measure the time-averaged outburst flux $\langle F \rangle$ (which is proportional to $\langle \dot{M} \rangle$). We integrate all counts with $> 5\sigma$ significance during the five year period Jan 1996–Jan 2001 (3.9×10^8 counts; we adopt a $\pm 10\%$ uncertainty), which includes ≈ 5 outbursts. If the flux of Aql X-1, when not in outburst, was always just below the RXTE/ASM 1-day detection limit (0.1 c/s), this would increase the time-average outburst flux by only 4%. Using W3PIMMS, the ASM counts/flux conversion for power-law spectra $\alpha=0.8, 1.0, 2.0$ are 3.4, 3.6, and $5.0 \times 10^{-10} \text{ ergs cm}^{-2} \text{count}^{-1}$ (0.5-10.0 keV), respectively. For blackbody spectra $kT=0.8\text{--}1.4$ keV, the conversion factors are approximately the same: $3.3 \times 10^{-10} \text{ ergs cm}^{-2} \text{count}^{-1}$. We adopt $3.6 \times 10^{-10} \text{ ergs cm}^{-2} \text{count}^{-1}$ (0.5-10.0 keV) with the realization that the spectral and bolometric uncertainties can be as large as $\sim 25\%$. This then gives $\langle F \rangle \approx 10^{-9} \text{ erg cm}^{-2} \text{s}^{-1}$, or roughly $\langle \dot{M} \rangle \approx 2.5 \times 10^{-10} M_{\odot} \text{ yr}^{-1} (d/5 \text{ kpc})^2$.

We assume that the NS liberates $GM/R \approx 1.8 \times 10^{20} \text{ erg g}^{-1}$ per accreted baryon during the outburst. Then, from equation (1), we expect a quiescent bolometric thermal flux $F_q \approx \langle F \rangle / 130$, or $F_q = 7.7 \times 10^{-12} \text{ erg cm}^{-2} \text{s}^{-1}$, compared with $F_{\text{bol}}^{\infty} = 2.5 \times 10^{-12} \text{ erg cm}^{-2} \text{s}^{-1}$ observed during the *Chandra* observation. The quiescent bolometric thermal flux is uncertain by $^{+0.35}_{-0.26}$ dex (about a factor of 2 in both directions, 1σ), and so is consistent with this prediction (BBR98; Eq. 1).

Note, on the other hand, that if one were to assume that 100% of the emergent luminosity were from accretion, this would set $\dot{M} = 1.1 \times 10^{-12} M_{\odot} \text{yr}^{-1}$, which is above the \dot{M} where gravity stratifies metals in the NS atmosphere – that is, where metal lines would become unobservable. We do not exclude the presence of metal lines in the observed spectrum, and it is possible that, at such an implied accretion rate, metal lines may be observed.

4. Discussion and Conclusions

We have detected Aql X–1 in quiescence, at a luminosity comparable to that observed in three previous epochs. This makes Aql X–1 the second transiently accreting, type-I X-ray bursting NS (after Cen X–4; Rutledge et al. 2001) which maintains a quiescent luminosity to within a factor of a few. The stability of Cen X–4’s quiescent luminosity over years, and the ability of Aql X–1 to return to the same quiescent luminosity between outbursts (where \dot{M} increases by more than a factor of 1000) are both strong support for their basal quiescent luminosity being set by deep crustal heating (BBR98). In addition, spectral evidence points to most of the quiescent emission being thermal emission from the NS surface.

While the H atmosphere spectral model implies a NS radius which is at the low end of the EOS range for the adopted distance (see, for example, Lattimer & Prakash (2001)), inclusion of an additional power-law component – although not statistically required – produces a systematically larger value of R_{∞} and smaller value of $kT_{\text{eff},\infty}$, which is the expected direction of bias if the previously observed power-law component is present. We therefore quote the best-fit value of $R_{\infty} = 13.4^{+5}_{-4}$ (d/5 kpc) km and $kT_{\text{eff},\infty} = 135^{+18}_{-12}$ eV which includes an $\alpha = 1$ power-law component, noting that these are not significantly different when we assume a value $\alpha = 2$. Greater scrutiny of the distances to this and similar objects is called for. Moreover, we examined the spectrum only in a limited range (0.5–8.0 keV), as *Chandra*/ACIS-S is not yet calibrated down to 0.2 keV.

However, puzzles remain. The quiescent X-ray luminosity of Aql X–1 has varied by a factor of 1.87 ± 0.21 over timescales of years, while remaining constant ($<15\%$ rms) on timescales 1–10,000 sec. This is similar to the intensity variability observed from another quiescent transient neutron star, Cen X–4, which has shown variability of a factor of ≈ 3 on timescales of days–yrs (Campana et al. 1997; Rutledge et al. 2000), and $<18\%$ rms variability on 1–10,000 sec timescales (Rutledge et al. 2000). In addition, the power-law spectral components in some of these sources cannot be explained as thermal emission; their origin is unclear.

A variation in $kT_{\text{eff},\infty}$ can be attributed to either a variation in quiescent accretion onto the compact object or a changing thermal emission. Since the NS core cannot change its temperature on these timescales, any variation in the thermal emission would need to be from either internal heat sources previously neglected (Ushomirsky & Rutledge 2001) or changes in the overlying envelope.

If quiescent accretion powers the variability in Cen X-4 and Aql X-1, then we are left with the surprising coincidence that \dot{M}_q provides a luminosity comparable to the deep crustal heating luminosity (Eq. 1), in at least two different systems. Even in its simplest form (a diminished accretion rate from a cool disk, King & Ritter 1998) it seems surprising that quiescent accretion would maintain near equality with the deep crustal heating luminosity. It seems even less likely if one invokes a magnetic propeller to regulate the accretion rate onto the NS in quiescence (Menou et al. 1999). Therefore, if the variability is due to accretion, it remains to be explained why the accretion rate provides a luminosity so nearly equal to that from deep crustal heating.

The authors are grateful to the *Chandra* Observatory team for producing this exquisite observatory. We thank the anonymous referee for comments which improved this paper. This research was partially supported by the National Science Foundation under Grant No. PHY99-07949 and by NASA through grant NAG 5-8658, NAG 5-7017 and the *Chandra* Guest Observer program through grant NAS GO0-1112B. L. B. is a Cottrell Scholar of the Research Corporation. E. F. B. acknowledges support from an Enrico Fermi Fellowship.

References

- Arnaud, K. A., 1996, in G. Jacoby & J. Barnes (eds.), *Astronomical Data Analysis Software and Systems V*, Vol. 101, p. 17, ASP Conf. Series
- Asai, K., Dotani, T., Hoshi, R., Tanaka, Y., Robinson, C. R., & Terada, K., 1998, PASJ 50, 611
- Asai, K., Dotani, T., Mitsuda, K., Hoshi, R., Vaughan, B., Tanaka, Y., & Inoue, H., 1996b, PASJ 48, 257
- Bildsten, L. & Rutledge, R. E., 2000, *The Neutron Star – Black Hole Connection*, Kouveliotou et al (eds.) (NATO ASI Elounda 1999); astro-ph/0005364
- Bildsten, L., Salpeter, E. E., & Wasserman, I., 1992, ApJ 384, 143
- Brandt, S., Castro-Tirado, A. J., & Lund, N., 1992, IAU Circ. 5664
- Brown, E. F., Bildsten, L., & Rutledge, R. E., 1998, ApJ 504, L95, [BBR98]
- Callanan, P. J., Filippenko, A. V., & Garcia, M. R., 1999, IAU Circ. 7086

- Campana, S., Colpi, M., Mereghetti, S., Stella, L., & Tavani, M., 1998a, *A&A Rev.* 8, 279
- Campana, S., Mereghetti, S., Stella, L., & Colpi, M., 1997, *A&A* 324, 941
- Campana, S., Stella, L., Mereghetti, S., Colpi, M., Tavani, M., Ricci, D., Fiume, D. D., & Belloni, T., 1998b, *ApJ* 499, L65
- Campana, S., Stella, L., Mereghetti, S., & Cremonesi, D., 2000, *A&A* 358, 583
- Chen, W., Shrader, C. R., & Livio, M., 1997, *ApJ* 491, 312
- Chevalier, C. & Ilovaisky, S. A., 1998, *IAU Circ.* 6806
- Chevalier, C., Ilovaisky, S. A., Leisy, P., & Patat, F., 1999, *A&A* 347, L51
- Colpi, M., Geppert, U., & Page, D., 2000, *ApJ* 529, L29
- Czerny, M., Czerny, B., & Grindlay, J. E., 1987, *ApJ* 312, 122
- Garcia, M. R., Callanan, P. J., McCarthy, J., Eriksen, K., & Hjellming, R. M., 1999, *ApJ* 518, 422
- Gorenstein, P., 1975, *ApJ* 198, 95
- Haensel, P. & Zdunik, J. L., 1990, *A&A* 227, 431
- Ilovaisky, S. A. & Chevalier, C., 1992a, *IAU Circ.* 5507
- Ilovaisky, S. A. & Chevalier, C., 1992b, *IAU Circ.* 5551
- Ilovaisky, S. A. & Chevalier, C., 1992c, *IAU Circ.* 5665
- Ilovaisky, S. A. & Chevalier, C., 1996, *IAU Circ.* 6416
- King, A. R. & Ritter, H., 1998, *MNRAS* 293, L42
- Lattimer, J. M. & Prakash, M., 2001, *ApJ* 550, 426
- Levine, A. M., Bradt, H., Cui, W., Jernigan, J. G., Morgan, E. H., Remillard, R., Shirey, R. E., & Smith, D. A., 1996, *ApJ* 469, L33
- McClintock, J. E., Horne, K., & Remillard, R. A., 1995, *ApJ* 442, 358
- Menou, K., Esin, A. A., Narayan, R., Garcia, M. R., Lasota, J. P., & McClintock, J. E., 1999, *ApJ* 520, 276
- Nayakshin, S. & Svensson, R., 2001, *ApJ* 551, L67
- Predehl, P. & Schmitt, J. H. M. M., 1995, *A&A* 293, 889
- Press, W., Flannery, B., Teukolsky, S., & Vetterling, W., 1995, *Numerical Recipes in C*, Cambridge University Press
- Rajagopal, M. & Romani, R. W., 1996, *ApJ* 461, 327
- Rutledge, R. E., Bildsten, L., Brown, E. F., Pavlov, G. G., & Zavlin, V. E., 1999, *ApJ* 514, 945
- Rutledge, R. E., Bildsten, L., Brown, E. F., Pavlov, G. G., & Zavlin, V. E., 2000, *ApJ* 529, 985
- Rutledge, R. E., Bildsten, L., Brown, E. F., Pavlov, G. G., & Zavlin, V. E., 2001, *ApJ* 551, 921
- Shakura, N. I. & Sunyaev, R. A., 1973, *A&A* 24, 337
- Thorstensen, J., Charles, P., & Bowyer, S., 1978, *ApJ* 220, L131

- Ushomirsky, G. & Rutledge, R. E., 2001, MNRAS, accepted, astro-ph/0101141
- Verbunt, F., Belloni, T., Johnston, H. M., Van der Klis, M., & Lewin, W. H. G., 1994, A&A 285, 903
- Weisskopf, M. C., 1988, *Space Science Reviews* 47, 47
- Welsh, W. F., Robinson, E. L., & Young, P., 2000, AJ 120, 943
- Zavlin, V. E., Pavlov, G. G., & Shibunov, Y. A., 1996, A&A 315, 141

Fig. 1.— The νF_ν model spectrum of Aql X–1, and the observed *Chandra*/ACIS-S BI data. The solid line is the best-fit *unabsorbed* (the intrinsic X-ray spectrum of Aql X–1, prior to absorption by the interstellar medium; see Table 1) H-atmosphere plus power-law model spectrum with $\alpha=1$ held fixed. The dashed-dotted line is the H-atmosphere component, and the dashed line is the power-law component. The two spectral components are equal near ≈ 3 keV, above which the power-law component dominates, and below which the H atmosphere component dominates. The crosses are the observed *Chandra* data, with error-bars in countrate.

Aql X-1: Chandra ACIS-S/BI (0.5–8.0 keV)

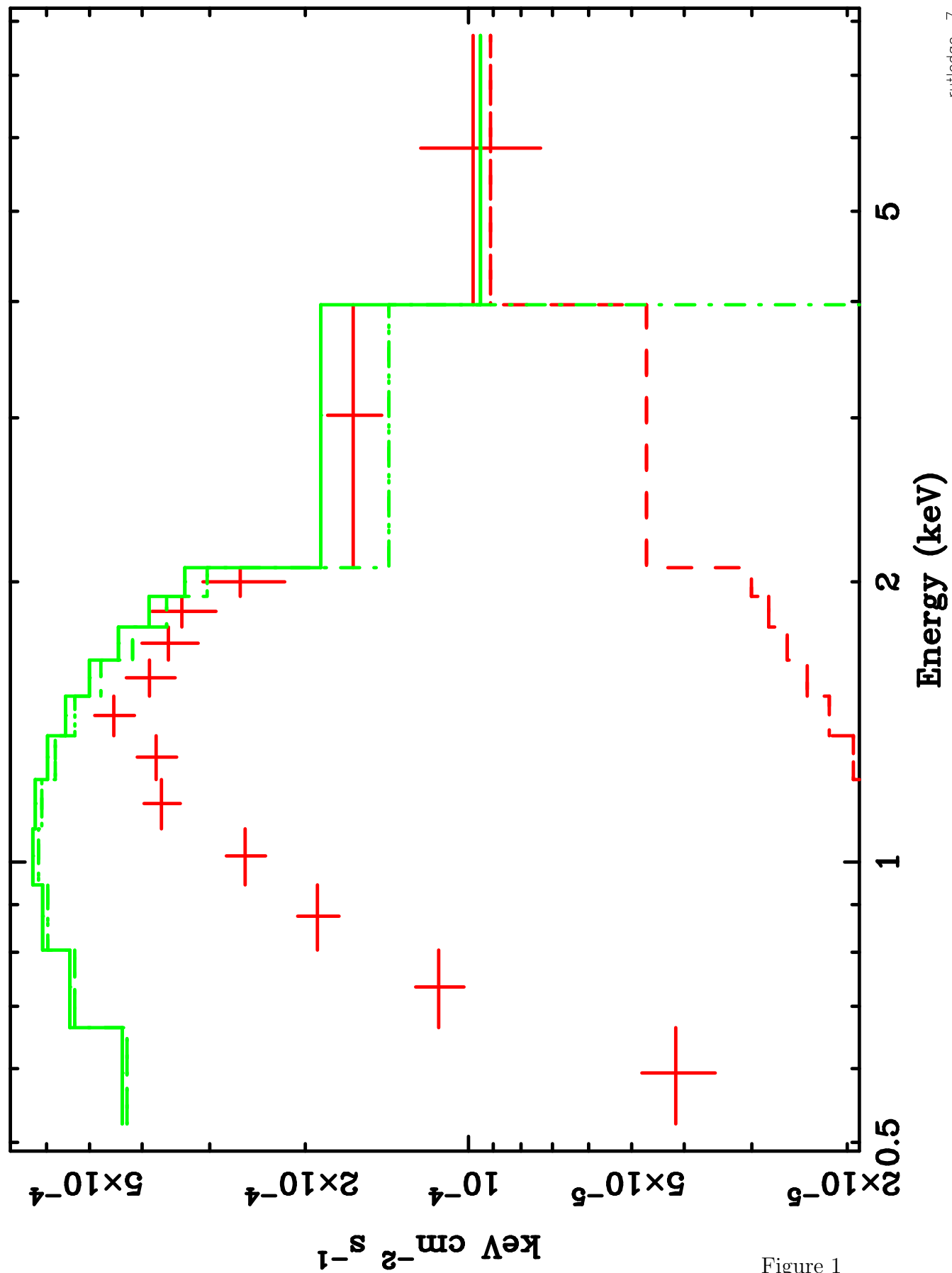


Figure 1

Table 1. *Chandra* Spectral Model Parameters (0.5-8 keV)

Parameter	Value
H Atmosphere	
$N_{\text{H},22}$	0.30 ± 0.06
$kT_{\text{eff},\infty}$ (eV)	156 ± 18
R_{∞} (km)	$9.4^{+2.7}_{-2.4}$
Total Model Flux	12
χ^2_{ν}/dof (prob)	1.7/10 (0.07)
H Atm. + Power Law ($\alpha = 1$)	
$N_{\text{H},22}$	$0.35^{+0.08}_{-0.07}$
$kT_{\text{eff},\infty}$ (eV)	135^{+18}_{-12}
R_{∞} (km)	13.4^{+5}_{-4}
α	(1.0)
$F_{X,PL}$	2.2 ± 1
Total Model Flux	14.7
χ^2_{ν}/dof (prob)	0.55/9 (0.84)
H Atm. + Power Law ($\alpha = 2$)	
$N_{\text{H},22}$	$0.36^{+0.10}_{-0.06}$
$kT_{\text{eff},\infty}$ (eV)	131 ± 19
R_{∞} (km)	13.8 ± 4
α	(2.0)
$F_{X,PL}$	$3.1^{+1.6}_{-1.4}$
Total Model Flux	14.9
χ^2_{ν}/dof (prob)	0.66/9 (0.72)
Photon Power Law	
$N_{\text{H},22}$	0.72 ± 0.09
α	4.1 ± 0.3
Total Model Flux	52^{+13}_{-10}
χ^2_{ν}/dof (prob)	1.4/10 (0.16)
Raymond-Smith	
$N_{\text{H},22}$	$0.47^{+0.06}_{-0.05}$
Z (Z_{\odot})	$< 5 \times 10^{-3}$
kT (keV)	0.77 ± 0.10
$\int n_e n_H dV \text{ cm}^{-3}$	$(1.8 \pm 0.4) \times 10^{57}$
Total Model Flux	19.4
χ^2_{ν}/dof (prob)	1.7/9 (0.08)
Multicolor Disk	
$N_{\text{H},22}$	$0.36^{+0.06}_{-0.05}$
T_{in} (keV)	0.43 ± 0.04
$R_{\text{in}} \sqrt{\cos(\theta)}$ km	$0.81^{+0.23}_{-0.17}$
Total Model Flux	14.0
χ^2_{ν}/dof (prob)	1.74/10 (0.06)
Blackbody	
$N_{\text{H},22}$	0.23 ± 0.06
$kT_{\text{eff},\infty}$ (eV)	330 ± 20
R_{∞} (km)	1.9 ± 0.3
Total Model Flux	10
χ^2_{ν}/dof (prob)	2.0/10 (0.03)

Note. — X-ray fluxes are un-absorbed, in units of $10^{-13} \text{ erg cm}^{-2} \text{ s}^{-1}$ (0.5-10 keV). Upper-limits and uncertainties are 90% confidence. Values in parenthesis are held fixed. Assumed source distance $d=5$ kpc.

Table 2: Observation List

Instrument	Obs. Date (dd/mm/year)	Days Since Outburst End	Days Since Outburst Start	Refs.
<i>ROSAT</i> /PSPC (1)	15/10/1992	110-130	190	1
<i>ROSAT</i> /PSPC (2)	24/03/1993	...	125	2, 3
<i>ASCA</i>	21/10/1996	70	130	2, 4
<i>Chandra</i>	28/11/2000	7	70	2

1, Ilovaisky & Chevalier 1992a; Ilovaisky & Chevalier 1992b; 2, RXTE/ASM; 3, Brandt et al. 1992; Ilovaisky & Chevalier 1992c; 4, Ilovaisky & Chevalier 1996

Table 3: Multi-Observation Spectral Fits

χ^2_ν/dof (prob)	$N_{\text{H},22}$	$kT_{\text{eff},\infty}$ (eV)	R_∞ (km)	α	F_X (PL) ^c	F_X (Therm) ^d	Variable Parameter	<i>Chandra</i> ^b	<i>ROSAT</i> PSPC (1) ^b	<i>ROSAT</i> PSPC (2) ^b	<i>ASCA</i> ^b
1.43/66 (0.01)	—	150^{+8}_{-11}	$9.8^{+1.6}_{-1.4}$	11 ^a	$N_{\text{H},22}$	0.28 ± 0.04	0.47 ± 0.06	0.20 ± 0.04	0.47 ± 0.06
0.98/66 (0.52)	0.26 ± 0.03	—	$8.3^{+0.6}_{-1.2}$	11 ^a	$kT_{\text{eff},\infty}$	164^{+10}_{-6}	145^{+9}_{-5}	168^{+12}_{-6}	153^{+10}_{-4}
0.96/66 (0.58)	0.26 ± 0.03	159^{+12}_{-7}	—	11 ^a	R_∞	$8.7^{+0.9}_{-1.5}$	$6.8^{+0.7}_{-1.1}$	$9.3^{+1.0}_{-1.6}$	$7.5^{+0.8}_{-1.3}$
1.0/64 (0.49)	—	120^{+10}_{-30}	$17.6^{+12.6}_{-3.7}$	$1.3^{+1.3}_{-1.0}$	2.6	12	$N_{\text{H},22}$	0.40 ± 0.08	$0.60^{+0.03}_{-0.09}$	0.32 ± 0.07	0.60 ± 0.06
0.62/64 (0.99)	$0.31^{+0.10}_{-0.04}$	—	$12.0^{+5.3}_{-2.3}$	0.80 ± 1.6	2.4	12 ^a	$kT_{\text{eff},\infty}$	143^{+10}_{-30}	127^{+15}_{-21}	148^{+10}_{-30}	134^{+8}_{-30}
0.60/64 (0.99)	$0.31^{+0.07}_{-0.02}$	141^{+14}_{-23}	—	$0.2^{+1.6}_{-1.9}$	2.5	12 ^a	R_∞	$11.6^{+4.6}_{-2.3}$	$9.1^{+3.2}_{-1.8}$	$12.5^{+4.8}_{-2.2}$	10 ± 1.8
0.71/64 (0.96)	0.55 ± 0.10	100 ± 30	16 ± 12	3.5 ± 0.5	—	5.3	$F_{X,PL}$	2.4	1.2	2.9	1.7

Uncertainties are 1σ . Assumed source distance $d=5$ kpc. Model fluxes are corrected for absorption, in units of $10^{-13} \text{ erg cm}^{-2} \text{ s}^{-1}$. ^a Value is for *Chandra* observation. ^b Labels refer to observations listed in Table 2. ^c Best-fit flux for the power-law component. ^d Best-fit Flux for the thermal component.